



Proarrhythmia in the p.Met207Val PITX2c-Linked Familial Atrial Fibrillation-Insights From Modeling

Jieyun Bai^{1*}, Yaosheng Lu¹, Andy Lo², Jichao Zhao^{2*} and Henggui Zhang^{3,4*}

¹ Department of Electronic Engineering, College of Information Science and Technology, Jinan University, Guangzhou, China, ² Auckland Bioengineering Institute, The University of Auckland, Auckland, New Zealand, ³ Biological Physics Group, School of Physics & Astronomy, University of Manchester, Manchester, United Kingdom, ⁴ Pilot National Laboratory for Marine Science and Technology, Qingdao, China

OPEN ACCESS

Edited by:

Futoshi Toyoda,
Shiga University of Medical
Science, Japan

Reviewed by:

Kunichika Tsumoto,
Kanazawa Medical University, Japan
Georges Christé,
Institut National de la Santé et de la
Recherche Médicale
(INSERM), France

*Correspondence:

Jieyun Bai
bai_jieyun@126.com
Jichao Zhao
j.zhao@auckland.ac.nz
Henggui Zhang
henggui.zhang@manchester.ac.uk

Specialty section:

This article was submitted to
Computational Physiology and
Medicine,
a section of the journal
Frontiers in Physiology

Received: 26 June 2019

Accepted: 30 September 2019

Published: 22 October 2019

Citation:

Bai J, Lu Y, Lo A, Zhao J and Zhang H
(2019) Proarrhythmia in the
p.Met207Val PITX2c-Linked Familial
Atrial Fibrillation-Insights From
Modeling. *Front. Physiol.* 10:1314.
doi: 10.3389/fphys.2019.01314

Functional analysis has shown that the p.Met207Val mutation was linked to atrial fibrillation and caused an increase in transactivation activity of PITX2c, which caused changes in mRNA synthesis related to ionic channels and intercellular electrical coupling. We assumed that these changes were quantitatively translated to the functional level. This study aimed to investigate the potential impact of the PITX2c p.Met207Val mutation on atrial electrical activity through multiscale computational models. The well-known Courtemanche-Ramirez-Nattel (CRN) model of human atrial cell action potentials (APs) was modified to incorporate experimental data on the expected p.Met207Val mutation-induced changes in ionic channel currents (I_{NaL} , I_{Ks} , and I_{Kr}) and intercellular electrical coupling. The cell models for wild-type (WT), heterozygous (Mutant/Wild type, MT/WT), and homozygous (Mutant, MT) PITX2c cases were incorporated into homogeneous multicellular 1D and 2D tissue models. Effects of this mutation-induced remodeling were quantified as changes in AP profile, AP duration (APD) restitution, conduction velocity (CV) restitution and wavelength (WL). Temporal and spatial vulnerabilities of atrial tissue to the genesis of reentry were computed. Dynamic behaviors of re-entrant excitation waves (Life span, tip trajectory and dominant frequency) in a homogeneous 2D tissue model were characterized. Our results suggest that the PITX2c p.Met207Val mutation abbreviated atrial APD and flattened APD restitution curves. It reduced atrial CV and WL that facilitated the conduction of high rate atrial excitation waves. It increased the tissue's temporal vulnerability by increasing the vulnerable window for initiating reentry and increased the tissue spatial vulnerability by reducing the substrate size necessary to sustain reentry. In the 2D models, the mutation also stabilized and accelerated re-entrant excitation waves, leading to rapid and sustained reentry. In conclusion, electrical and structural remodeling arising from the PITX2c p.Met207Val mutation may increase atrial susceptibility to arrhythmia due to shortened APD, reduced CV and increased tissue vulnerability, which, in combination, facilitate initiation and maintenance of re-entrant excitation waves.

Keywords: atrial fibrillation, PITX2c, modeling and simulation, human atrial action potential model, electrical and structural remodeling, gene regulation, transcription factors, single nucleotide polymorphism

INTRODUCTION

The most common arrhythmia atrial fibrillation (AF) increases with age and is associated with adverse events (such as heart failure, stroke, hypertension and diabetes) (Heijman et al., 2018). These cardiac disorders are thought to promote AF which is characterized by uncoordinated patterns of atrial electrical activation and a fast and irregular heartbeat (Hansen et al., 2015). Whilst the precise mechanisms underlying AF are complex and poorly understood, AF-induced ionic remodeling and structural cardiac diseases are major factors in initiating and sustaining AF (Grandi et al., 2011; Colman et al., 2013; Koivumäki et al., 2014). However, genome-wide association studies suggested genetic variation contributes to AF susceptibility, with >100 AF-associated loci reported to date (Nielsen et al., 2018), including the atrial-selective transcription factor PITX2 (paired like homeodomain-2) that regulates membrane effector genes associated with AF (Gudbjartsson et al., 2007; Chinchilla et al., 2011; Kirchhof et al., 2011; Qiu et al., 2014; Tao et al., 2014; Lozano-Velasco et al., 2015; Pérez-Hernández et al., 2015; Bai et al., 2018; Mechakra et al., 2019). In these studies, Mechakra et al. (2019) identified a non-synonymous mutation c.619A>G (p.Met207Val, rs138163892) of PITX2. Functional analysis of the transactivation activity of wild-type and variant PITX2c revealed a gain-of-function of PITX2c (the PITX2c isoform), leading to an increase in the mRNA level of KCNH2 (the α subunit of I_{Kr}), KCNQ1 (the α subunit of I_{Ks}), SCN1B (the β 1 subunit of sodium channels that modulates I_{NaL}), GJA5 (Cx40), and GJA1 (Cx43) (Mechakra et al., 2019).

I_{Kr} , I_{Ks} , and I_{NaL} regulate late repolarization of action potentials (APs), and Cx40 and Cx43 mediate intercellular electrical coupling via gap junctions (Dhillon et al., 2014). Ionic remodeling due to changes in potassium currents (Caballero et al., 2010; González de la Fuente et al., 2012; Pérez-Hernández et al., 2015) and I_{NaL} (Sossalla et al., 2010), and structural remodeling arising from abnormalities in Cx40 and Cx43 (Polontchouk et al., 2001; Nao et al., 2003; Wetzal et al., 2005) have been found in chronic AF patients. In a previous experimental study, it has been shown that overexpression of PITX2c (a gain-of-function) increased I_{Ks} density and decreased I_{CaL} density in atrial myocytes from chronic AF patients (Pérez-Hernández et al., 2015). These changes could contribute to the long-term stabilization of the arrhythmia by shortening the AP duration (APD) (González de la Fuente

et al., 2012). By contrast, whilst the gain-of-function arising from the p.Met207Val mutation has been suggested to increase susceptibility to familial AF (Mechakra et al., 2019), this link remains to be demonstrated directly.

The mechanisms by which ionic and structural remodeling induced by the PITX2c p.Met207Val mutation promotes and perpetuates AF have not yet been elucidated. Complex electrical wave dynamics observed during AF is determined by AP morphology, APD, conduction velocity (CV) restitution, wavelength (WL), vulnerable window (VW) for unidirectional conduction block, and the minimal substrate size required to induce re-entry (Bai et al., 2016b; Ni et al., 2017; Whittaker et al., 2017, 2018a,b). Therefore, utilizing a multi-scale computational model of the human atria based on experimental data on the PITX2c p.Met207Val mutation, we simulated electrical activity to quantify its potential impact at the cellular, 1D fiber tissue and 2D sheet tissue levels.

METHODS

Human Atrial Action Potential Model

The Courtemanche-Ramirez-Nattel (CRN) model (Courtemanche et al., 1998) of the human atrial AP was chosen to investigate the proarrhythmic effects of the PITX2c p.Met207Val mutation, because this model was suggested to study spatiotemporal characteristics of atrial fibrillation at the tissue and organ levels (Seemann et al., 2006; Kharche et al., 2012). The original CRN model was modified to reflect the observed kinetic properties of the I_{NaL} current (Figure 1A) that was based on the work of Grandi et al. (2011), who developed it using experimental data from human atrial myocardium (Sossalla et al., 2010). This I_{NaL} model is given by:

$$I_{NaL} = G_{NaL} \times m^3 \times h \times (V_m - E_{Na}) \quad (1)$$

$$\frac{dh}{dt} = \frac{h_{\infty} - h}{\tau_h} \quad (2)$$

$$h_{\infty} = \frac{1.0}{1.0 + \exp((V_m + 91)/6.1)} \quad (3)$$

$$\tau_h = 600 \text{ ms} \quad (4)$$

$$\frac{dm}{dt} = \frac{m_{\infty} - m}{\tau_m} \quad (5)$$

$$m_{\infty} = \frac{\alpha_m}{\alpha_m + \beta_m} \quad (6)$$

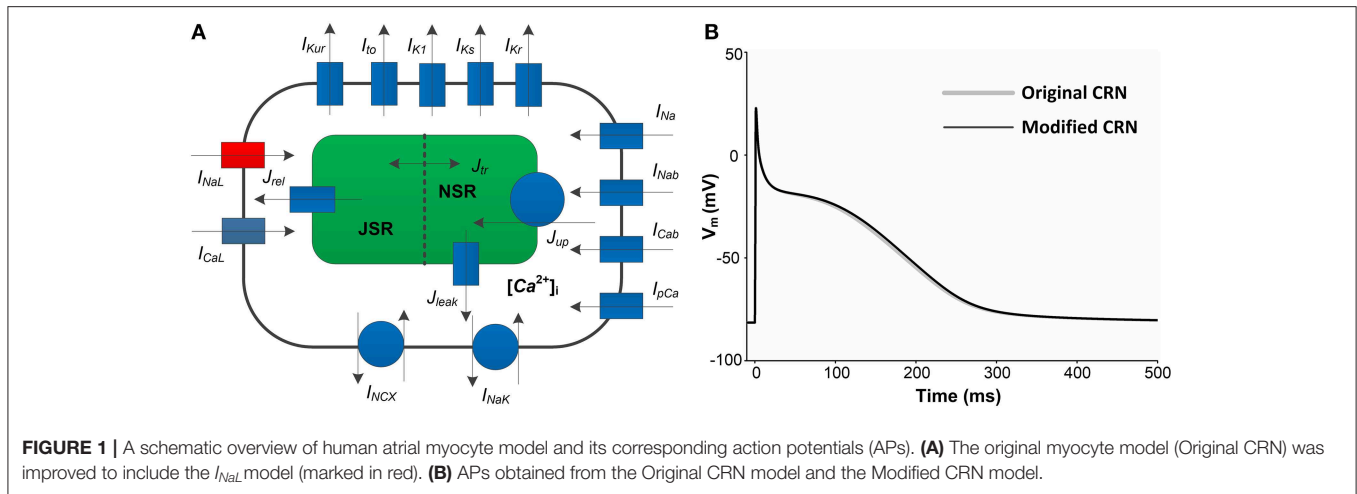
$$\tau_m = \frac{1}{\alpha_m + \beta_m} \quad (7)$$

$$\alpha_m = \frac{0.32 (V_m + 47.13)}{1.0 - \exp(-0.1 (V_m + 47.13))} \quad (8)$$

$$\beta_m = 0.08 \exp(-V_m/11) \quad (9)$$

where G_{NaL} (0.0025 nS/pF) is the maximal conductance, m and h are two gate variables for I_{NaL} , V_m is the membrane potential, and E_{Na} is the sodium equilibrium potential. m_{∞} and h_{∞} denote steady-state activation and steady-state inactivation, respectively. τ_m/τ_h is the time constant for m_{∞}/h_{∞} .

Abbreviations: 1D and 2D, one- and two-dimensional model; AF, Atrial fibrillation; AP, Action potential; APD, Action potential duration; APDR, APD restitution; APD₅₀, APD values at 50% repolarization; APD₉₀, APD values at 90% repolarization; APA, AP amplitude; BCL, Basic cycle length; CV, Conduction velocity; CVR, CV restitution; CRN model, Courtemanche-Ramirez-Nattel model of electrical action potential of human atrial cells; D, Diffusion coefficient; DI, Diastolic interval; dV/dt_{max}, Maximum depolarization rate; ERP, Effective refractory period; Grandi model, Grandi model of electrical action potential of human atrial cells; I_{CaL} , L-type calcium current; I_{NaL} , Late sodium current; I_{Ks} , The slow delayed rectifier potassium current; I_{Kr} , The rapid delayed rectifier potassium current; MT, Mutant PITX2c; MT/WT, Mutant/Wild type PITX2c; PITX2, Paired like homeodomain-2; PITX2c, PITX2c isoform; RMP, Resting membrane potential; VW, Vulnerable window; WL, Wavelength; WT, Wild-type PITX2c.



Thus, the modified CRN model is described as

$$\frac{dV_m}{dt} = -\frac{I_{ion} + I_{stim}}{C_m} \quad (10)$$

$$I_{ion} = I_{Na} + I_{NaL} + I_{CaL} + I_{Nab} + I_{Cab} + I_{pCa} + I_{to} + I_{Kr} + I_{Ks} + I_{Kur} + I_{NCX} + I_{NaK} \quad (11)$$

where I_{ion} is the sum of all ionic currents, I_{stim} (with a duration of 0.5 ms and a strength of -80 pA/pF) is the external stimulus current and C_m (100 pF) is the total membrane capacitance. Compared with the original CRN model, the amplitude, duration, and shape of the AP obtained from the modified CRN model had no significant changes (**Figure 1B**). All the equations, parameter values and initial conditions necessary to carry out the single cell simulations in this study can be found in the **Supplementary Table 1**.

The modified CRN model was used to investigate the characteristics of APs. These AP features included resting membrane potential (RMP), AP amplitude (APA), the maximum depolarization rate (dV/dt_{max}), AP duration at 50% repolarization (APD_{50}), AP duration at 90% repolarization (APD_{90}) and APD restitution (APDR). APDR was measured by using the standard dynamic method. The human atrial myocyte was firstly paced at a basic cycle length (BCL) of 1,000 ms for 700 beats to achieve steady-state APD_{90} s and then the BCL was progressively reduced by 5 to 50 ms. APDR curves were generated by plotting APD_{90} vs. diastolic interval (DI) which was computed as BCL minus APD_{90} .

Modeling Electrical and Structural Remodeling Due to the PITX2c p.Met207Val Mutation

To obtain human atrial myocyte models that reproduced the experimentally observed changes in the mRNA levels corresponding to key proteins under wild-type (WT), heterozygous (Mutant/Wild type PITX2c, MT/WT) and homozygous (Mutant PITX2c, MT) conditions (Mechakra et al., 2019), we assumed that these changes in mRNA expression are quantitatively reflected at the final functional level of

TABLE 1 | The PITX2c p.Met207Val mutation-induced changes (%) in structural and electrical components.

	Wild-type (WT)	Heterozygous expression (MT/WT)	Homozygous expression (MT)
I_{NaL} (%)	100	190	170
I_{Ks} (%)	100	100	180
I_{Kr} (%)	100	260	360
D (%)	100	80	76

The reduction rate of the diffusive coefficient was determined by the $Cx43/[Cx43+Cx40]$ ratio. Under the WT condition, the $Cx43:Cx40$ ratio is 1:1, so the $Cx43/[Cx43+Cx40]$ ratio is 0.5 and D (%) is set to be 100%. According to experimental data on mRNA levels of $Cx43$ and $Cx40$, D (%) is set to be 80% and 76%, respectively, under MT/WT and MT conditions. Bold values represent parameters and characteristics under the p.Met207Val PITX2c mutation condition.

ion channels and connexins. Therefore, we changed the maximal conductances of I_{NaL} , I_{Ks} and I_{Kr} to account for ionic remodeling due to the PITX2c p.Met207Val mutation, and altered the diffusion coefficient (D) to simulate the effects of changed intercellular electrical coupling via gap junctions ($Cx43$ and $Cx40$). According to the work of Kanagaratnam et al. (2002), the $Cx43/[Cx40+Cx43]$ ratio is associated with intercellular electrical coupling and conduction velocity (CV), such that, as the proportion of $Cx40$ signal increased (and that for $Cx43$ decreased), the CV decreased. Therefore, the $Cx43/[Cx40+Cx43]$ ratio was used to change the parameter D . In our study, two different cases (i.e., MT/WT and MT) were considered for PITX2c p.Met207Val mutation-induced changes in I_{NaL} , I_{Ks} , I_{Kr} , and D (**Table 1**).

Multicellular Atrial Tissue Models

These developed human atrial myocyte models were incorporated into 1D and 2D multicellular atrial tissue models with the modification to D for representing structural remodeling. These multicellular models were described by the following partial differential equation

$$C_m \frac{\partial V_m}{\partial t} = -I_{ion} + \nabla D \nabla V_m \quad (12)$$

where D is a tensor describing the conductivity of the tissue and ∇ is a gradient or Laplacian operator. In one dimension, $D = 0.031 \text{ mm}^2/\text{ms}$; in two dimensions, $D_{ij} = 0.031 \text{ mm}^2/\text{ms}$ for $i = j$, and $D_{ij} = 0.0 \text{ mm}^2/\text{ms}$ for $i \neq j$. The surface to volume ratio is 1 and C_m is 100 pF. These values, in the WT case, which can lead to a planar wave with a CV of 0.269 mm/ms. Time (t) and space (x) steps were set to be 0.005 ms and 0.1 mm, respectively.

In the present study, we designed three idealized geometries (a 1D cable model with 375 nodes, a 2D sheet model with 375×375 nodes and a homogeneous 2D tissue model with 750×750 nodes). In these models, the 1D cable was used to generate CV restitution (CVR) curves, and to measure CV, WL, and VW. CVR was measured by using the standard dynamic method. The 1D cable was paced at a BCL of 1,000 ms for 50 beats to achieve steady-state AP wavefronts and then the BCL was progressively reduced by 50 ms. CVR curves were constructed by plotting CV against BCL. WL was computed as the product of CV and effective refractory period (ERP). ERP and VW were calculated by using the extra stimulus method. Propagating AP wavefronts were evoked by an S1 stimulus at a BCL of 1,000 ms for 50 beats and then a test S2 stimulus applied during the refractory tail of the 50th AP wave after a time delay (S1-S2 time interval). The maximal S1-S2 interval to fail to excite AP waves (bidirectional block) was defined as ERP in atrial tissues. The time window between the maximal S1-S2 interval for bidirectional block and the minimal S1-S2 interval for bidirectional conduction was defined as VW to induce unidirectional conduction block.

In addition to the temporal vulnerability of atrial tissues quantified by VW, the spatial vulnerability was evaluated in the homogeneous 2D tissue model with 750×750 nodes using an S1-S2 protocol. A planar wave evoked by an S1 stimulus propagated from the left side to the right side. Once this wave had passed over the first half of the domain, an S2 stimulus was applied to a center region with the same width (1.0 mm) and different lengths. The minimal substrate size was defined as the minimal size of the S2 stimulus necessary to form and sustain reentry.

To further investigate the temporal-spatial characteristics of electrical waves due to the PITX2c p.Met207Val mutation, we used the standard S1-S2 protocol to induce spiral waves in the homogeneous 2D tissue model with 375×375 nodes. A planar S1 stimulus was applied to the left boundary to initiate a planar wave. During the VW, a rectangular S2 stimulus was applied to the top left quarter of the domain to initiate a spiral wave. The life span of the spiral wave was measured as the time duration from initiation to dissipation. The tip meander path was traced with the method of Fenton and Karma (Fenton and Karma, 1998). Dominant frequencies of action potential (AP) profiles obtained from the central point of the domain were computed using the Fast Fourier Transform technique (Bai et al., 2016a, 2017a,b).

RESULTS

Effects of the PITX2c p.Met207Val Mutation on the Human Atrial Action Potential

Based on the experimental study of Mechakra et al. (2019), simulations of the functional impact of an increased transactivation activity of PITX2c due to the p.Met207Val

mutation on Cx43, Cx40, I_{NaL} , I_{Ks} , and I_{Kr} were conducted to investigate how they contribute to atrial electrical and structural abnormalities. **Figure 2A** shows the relative changes caused by the gain-of-function mutation p.Met207Val (MT) include an increase in I_{NaL} (1.7-fold), I_{Ks} (1.8-fold), and I_{Kr} (3.6-fold) and a reduction in the Cx43/[Cx40+Cx43] ratio (0.76-fold).

This ionic remodeling (I_{NaL} , I_{Ks} , and I_{Kr}) arising from the PITX2c p.Met207Val mutation abbreviated human atrial APD₉₀ as shown in **Figure 2B**. The measured APD₉₀ was 260.62 ms for the WT condition, which was shortened to 197.58 ms for the MT/WT condition and to 170.14 ms under the MT condition. APA, dV/dt_{max} and RMP under the MT condition showed no significant changes as compared to the WT condition. The most obvious change of AP due to the electrical remodeling induced by the mutation was the APD shortening.

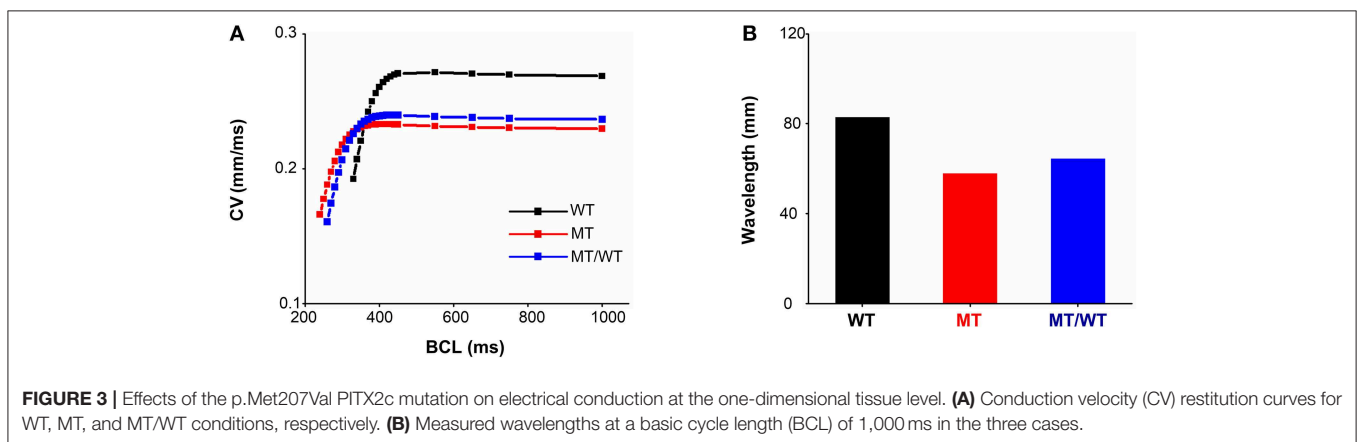
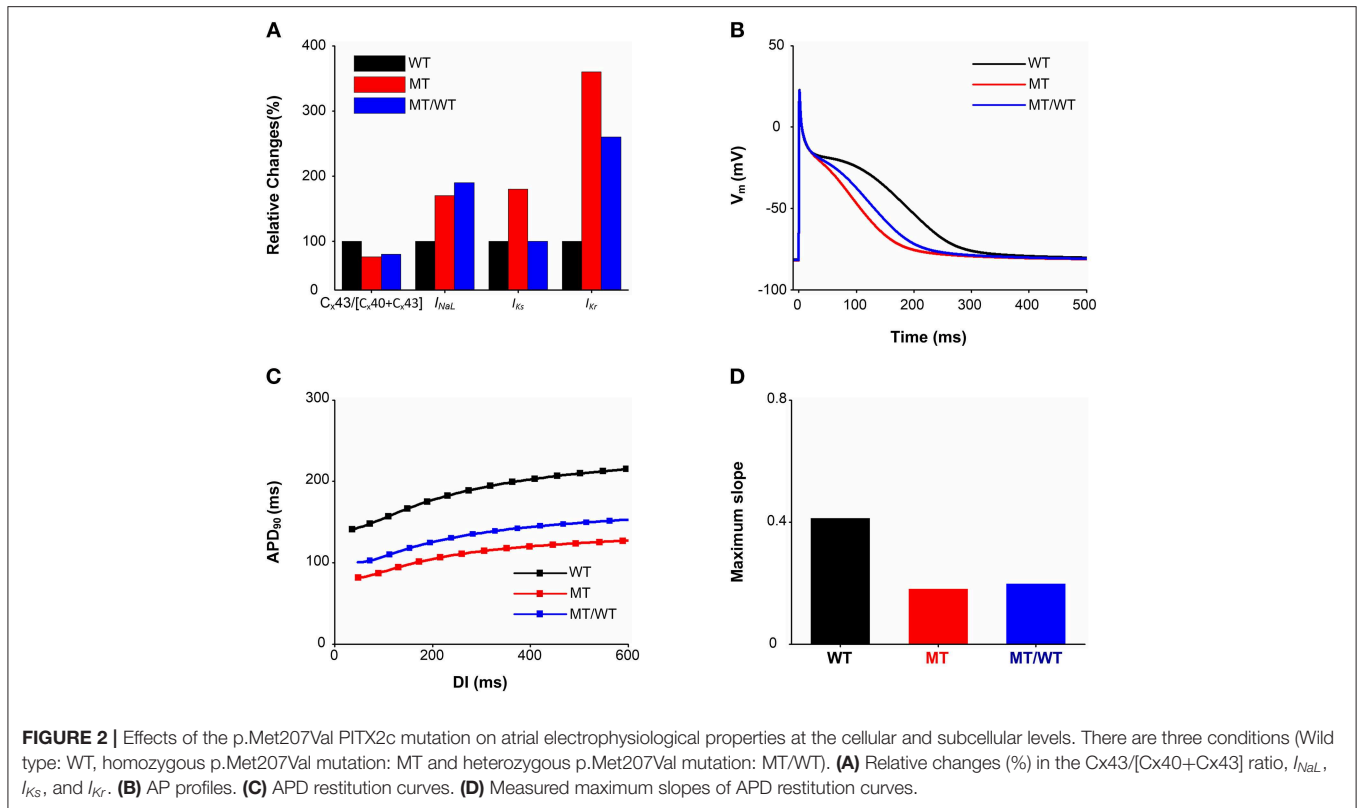
The APD shortening in the MT/WT and MT conditions was also rate-dependent as shown in **Figure 2C**. Across a range of DIs, the measured APD_{90s} under MT/WT and MT conditions were smaller compared to the WT condition. APD restitution curves plotted by APD₉₀ vs. DI were downshifted and flattened by the PITX2c p.Met207Val mutation. The computed maximal slope (0.41) for the WT condition was reduced to 0.20 and 0.18 under MT/WT and MT conditions, respectively (**Figure 2D**). APD shortening and flattened APD restitution curve implied that the PITX2c p.Met207Val mutation enabled human atrial cells to support electrical activity to persist at high rates.

Effects of the PITX2c p.Met207Val Mutation on Electrical Conduction at the 1D Tissue Level

In addition to ionic remodeling, structural remodeling associated with reduced intercellular coupling due to the PITX2c p.Met207Val mutation was incorporated into atrial tissue models. Using a 1D cable model, we computed CVR and WL under the WT, WT/MT, and MT conditions (**Figure 3**). At a BCL of 1,000 ms, the measured CV was decreased from 0.269 mm/ms for the WT condition to 0.237 and 0.230 mm/ms, under the WT/MT and MT conditions, respectively. The PITX2c p.Met207Val mutation downshifted CVR curves (**Figure 3A**) and facilitated electrical conduction at higher rates compared to the WT condition. The computed maximum rate of an electrical wave was increased from 194 beats/min for the WT condition to 220 and 238 beats/min, under MT/WT and MT conditions, respectively. WL abbreviation was also observed under mutant conditions (**Figure 3B**). The measured WL at a BCL of 1,000 ms was 82.72, 64.11, and 57.73 mm, for WT, MT/WT and MT conditions, respectively. Changes in CV and WL implied that the PITX2c p.Met207Val mutation allowed electrical waves to maintain in smaller tissue sizes that could occur under the WT condition.

Effects of the PITX2c p.Met207Val Mutation on Temporal and Spatial Vulnerabilities of Atrial Tissue

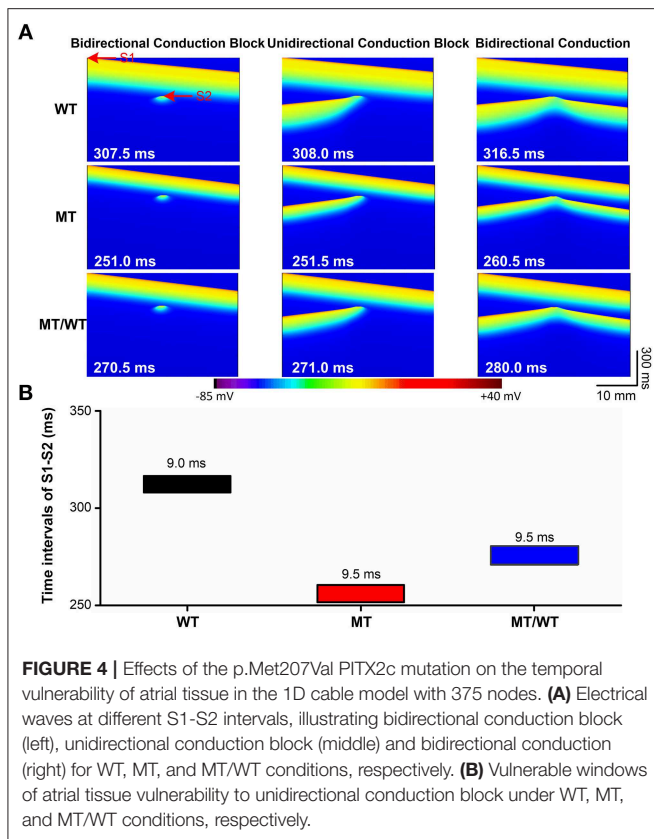
The PITX2c p.Met207Val mutation led to an increase in the atrial tissue's temporal vulnerability to unidirectional conduction block indexed by VW as shown in **Figure 4**. Under the WT



condition, the maximal S1-S2 interval for the generation of bidirectional conduction block was 307.5 ms and the minimal S1-S2 interval to induce bidirectional conduction was 316.5 ms. When S1-S2 time interval (e.g., 308.0 ms) was between 307.5 and 316.5 ms, unidirectional conduction block was induced (Figure 4A, top panel). The PITX2c p.Met207Val mutation decreased the S1-S2 time intervals, for bidirectional conduction block and bidirectional conduction, respectively (Figure 4A, middle and bottom panels). However, the width of VW was increased by the mutation (Figure 4B). The measured VW for the WT condition was 9.0 ms, which was increased to 9.5 ms for MT/WT and MT conditions.

The PITX2c p.Met207Val mutation caused an increase in the atrial tissue's spatial vulnerability to spiral wave formation. As shown in Figure 5A (top panel), under the WT condition, a planar wave was initiated by an S1 stimulus (time = 10 ms) and an S2 stimulus (time = 380 ms) with the minimal substrate size of 54 mm could result in sustaining reentry (time = 630 ms). The minimal substrate size was significantly decreased by the mutation from 54 to 47 and 36 mm, under MT/WT and MT conditions, respectively (Figure 5B).

Changes in VW and the minimal substrate size implied that the PITX2c p.Met207Val mutation may increase the likelihood of reentry formation.



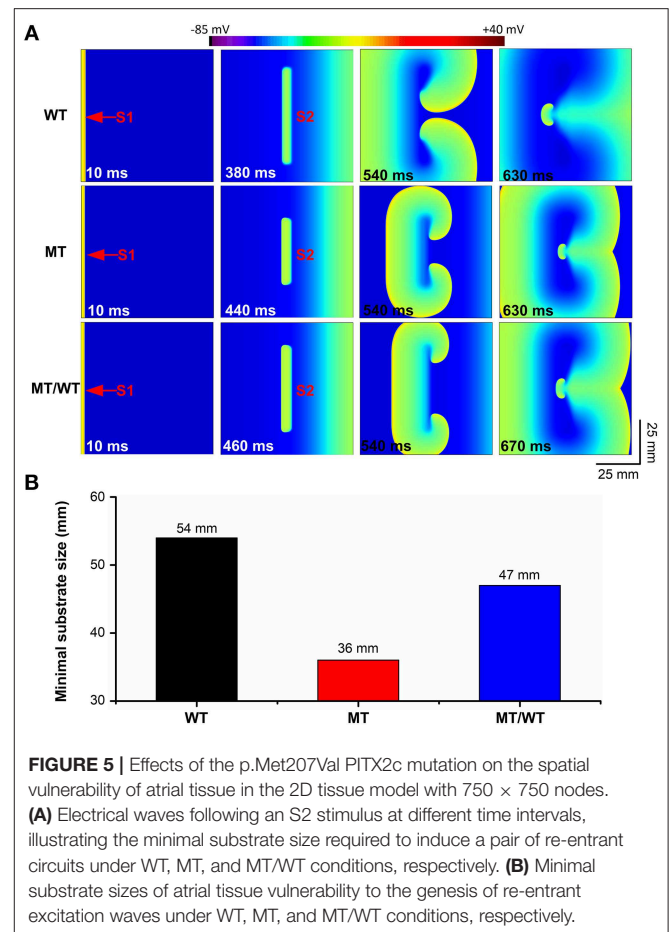
Effects of the PITX2c p.Met207Val Mutation on Spiral Wave Re-entry

To further examine whether the PITX2c p.Met207Val mutation promotes and perpetuates familial AF, its effects on the temporal-spatial dynamics of spiral waves were investigated. **Figure 6A** shows that the mutation led to the slow propagation of planar waves (time = 50 ms) and facilitated stable rotation (time = 4,000 ms) compared with the WT condition. The life span of the spiral wave was <2,000, >5,000 and >5,000 ms, under WT, MT/WT, and MT conditions, respectively. The meander area of the re-entrant wave trajectory under the MT condition was smaller than in the WT condition (**Figure 6B**). And the dominant oscillatory frequency of the membrane potential oscillations (**Figure 6C**) obtained from the marked point (**Figure 6A**, left panel) was increased from <4.0 Hz for the WT condition to 5.4 and 10.0 Hz, under the MT/WT and MT conditions, respectively (**Figure 6D**). Changes in life span, trajectory and dominant frequency of spiral waves implied that the PITX2c p.Met207Val mutation may increase the likelihood of familial AF (see **Supplementary Videos 1–3** for details).

A quantitative summary of the proarrhythmic effects of the PITX2c p.Met207Val mutation on human atrial electrical activity is listed in **Table 2**.

Action Potential Simulations With an Alternative Human Atrial Cell Model

To avoid model dependence of simulation results, we performed AP simulations using the Grandi et al. (Grand) model (Grandi

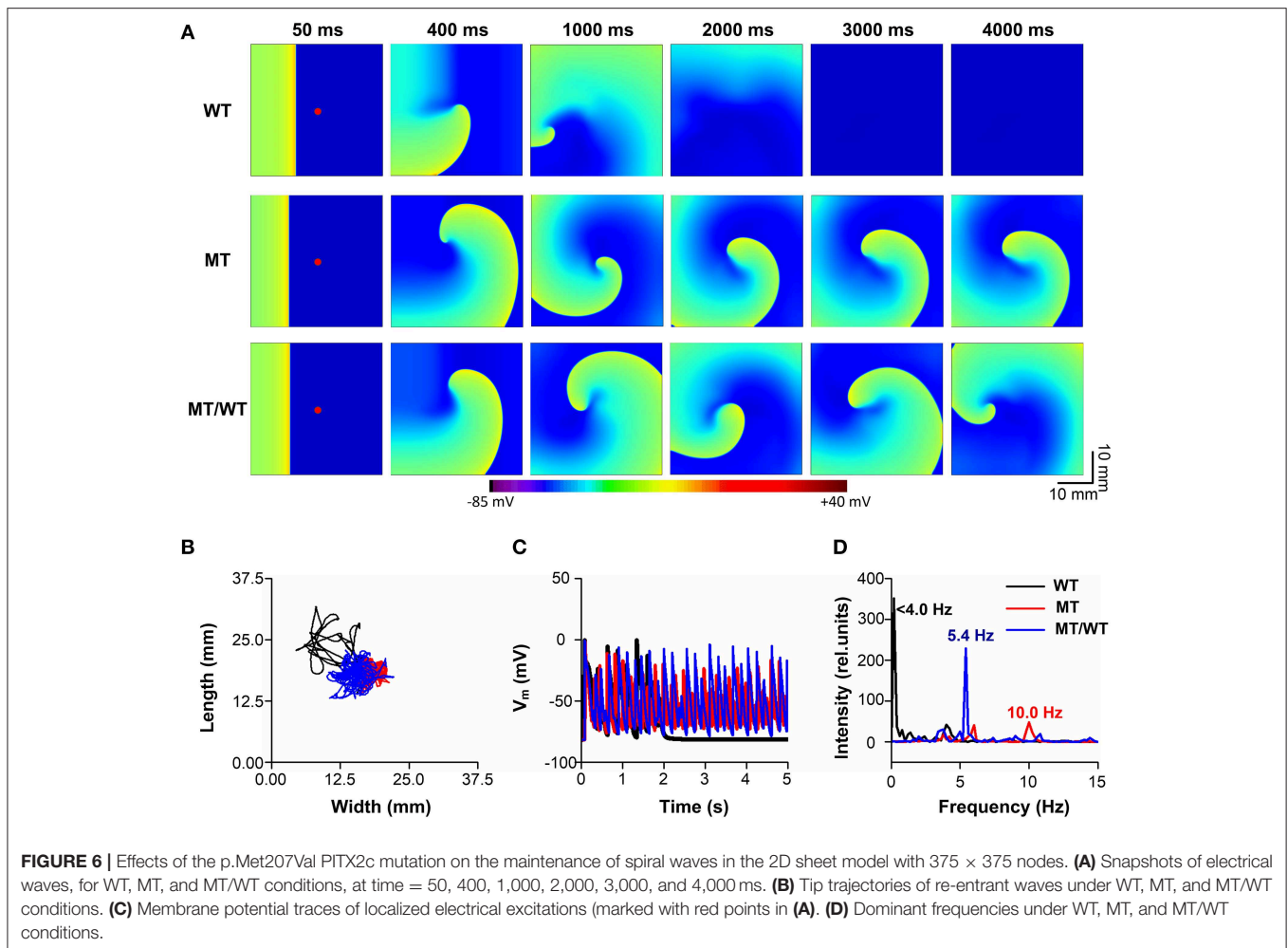


et al., 2011). The abbreviated APD (**Figures 7A,B**) and the flattened APD restitution curve (**Figure 7C**) under the MT condition were observed. This mutation-induced changes in AP obtained from the Grandi model was qualitatively similar to that from the modified CRN model. APA, dV/dt_{max} and RMP under the MT condition showed no significant changes as compared to the WT condition (**Table 3**). In addition, the maximal slope of the APD restitution curve was reduced from 20.70 under the WT condition to 5.90 and 4.16, under MT/WT and MT conditions, respectively (**Figure 7D**).

DISCUSSION

Main Findings

To our knowledge, this is the first study to investigate mechanisms underlying the generation and maintenance of re-entrant arrhythmias arising from the PITX2c p.Met207Val mutation (Mechakra et al., 2019). Our major findings are as follows: (1) This mutation-induced electrical remodeling abbreviated APD and flattened APDR curves. (2) The combined effects of electrical and structural remodeling due to the PITX2c p.Met207Val mutation slowed CV and shortened WL. (3) It increased atrial tissue vulnerability to initiation and maintenance of reentry by decreasing the substrate size to induce the figure-of-eight reentry and by increasing VW for unidirectional



conduction block. (4) It allowed electrical waves to maintain in smaller tissue sizes at higher rates. Consequently, these findings demonstrate that the PITX2c p.Met207Val mutation may increase the likelihood of familial AF due to increased atrial tissue's temporal and spatial vulnerabilities, which facilitate genesis and maintenance of re-entrant excitation waves.

Mechanisms of Familial Atrial Fibrillation Due to the PITX2c p.Met207Val Mutation

The increase of PITX2c expression or PITX2c activity has been linked to AF, as seen in the left atrium (Gore-Panter et al., 2014) and right atrial myocytes (Pérez-Hernández et al., 2015) from AF patients. In the case of the PITX2c p.Met207Val mutation, this variant was identified in 1 of 60 French patients with early-onset AF and its transactivation activity was increased 3.1-fold (Mechakra et al., 2019). In turn, this gain-of-function caused electrical and structural remodeling by modulating the mRNA levels corresponding to key proteins in AF (Mechakra et al., 2019). Although the causal link between atrial remodeling and the increased risk of AF has been demonstrated in previous modeling studies (Grandi et al., 2011; Colman et al., 2013; Koivumäki et al., 2014), the mechanisms underlying familial

AF associated with the PITX2c p.Met207Val mutation were not addressed directly.

In the present study, the genesis of AF in patients with the PITX2c p.Met207Val mutation may be attributable to APD shortening due to electrical remodeling and slow conduction resulted from structural remodeling. Electrical remodeling in our models included up-regulation in I_{NaL} , I_{Ks} , and I_{Kr} . Although upregulated I_{NaL} led to APD prolongation (Sossalla et al., 2010), the increase in I_{Ks} and I_{Kr} was found to play an important role in APD shortening (Kanaporis et al., 2019), resulting in an abbreviated WL of excitation waves that facilitated the initiation and maintenance of re-entry. Structural remodeling was modeled by decreasing the diffusion coefficient to simulate the reduced Cx43/(Cx43+Cx40) ratio. The reduction in the Cx43/(Cx43+Cx40) ratio caused slow conduction (Kanagaratnam et al., 2002; Beauchamp et al., 2006), leading to WL shortening and excitation waves at higher rates. The combined impact of electrical and structural remodeling on initiation and maintenance of atrial fibrillation can be characterized by atrial tissue's vulnerabilities to re-entry.

Effects of the PITX2c p.Met207Val mutation on the temporal and spatial vulnerabilities of atrial tissue contributed to the

increased susceptibility to familial AF. According to the leading circle concept (Allessie et al., 1977), functional re-entry pathways during AF naturally assume a path length equal to the minimum circuit size for re-entry, quantified mathematically as the wavelength (or product of refractoriness and conduction velocity) (Wiener, 1946). The wavelength is therefore expected to indicate average functional re-entry circuit size. Since the

maintenance of AF depends on the presence of a number of simultaneous reentering waves, and the minimum size of a reentrant wave is related to the wavelength, the wavelength should be an important determinant of the occurrence of AF. The spatial vulnerability of the atrial tissue (or the minimum length of the functional pathway necessary to sustain re-entry) was measured reciprocally by the minimal substrates to sustain re-entry (Kharche et al., 2012). In our modeling study, the formation of the induced reentrant excitation wave was dependent on the spatial size of the premature stimulus. We therefore measured the minimal size of the premature stimulus that enabled the formation of re-entry, as this is correlated with the wavelength of excitation (Kharche et al., 2012), and measures the minimal size of atrial substrate necessary to sustain re-entry. In our simulations, the PITX2c p.Met207Val mutation increased the spatial vulnerability of atrial tissue by decreasing the substrate size and WL due to abbreviated ERP and reduced CV. On the

TABLE 2 | A quantitative summary of the proarrhythmic effects of the PITX2c p.Met207Val mutation on human atrial electrical activity.

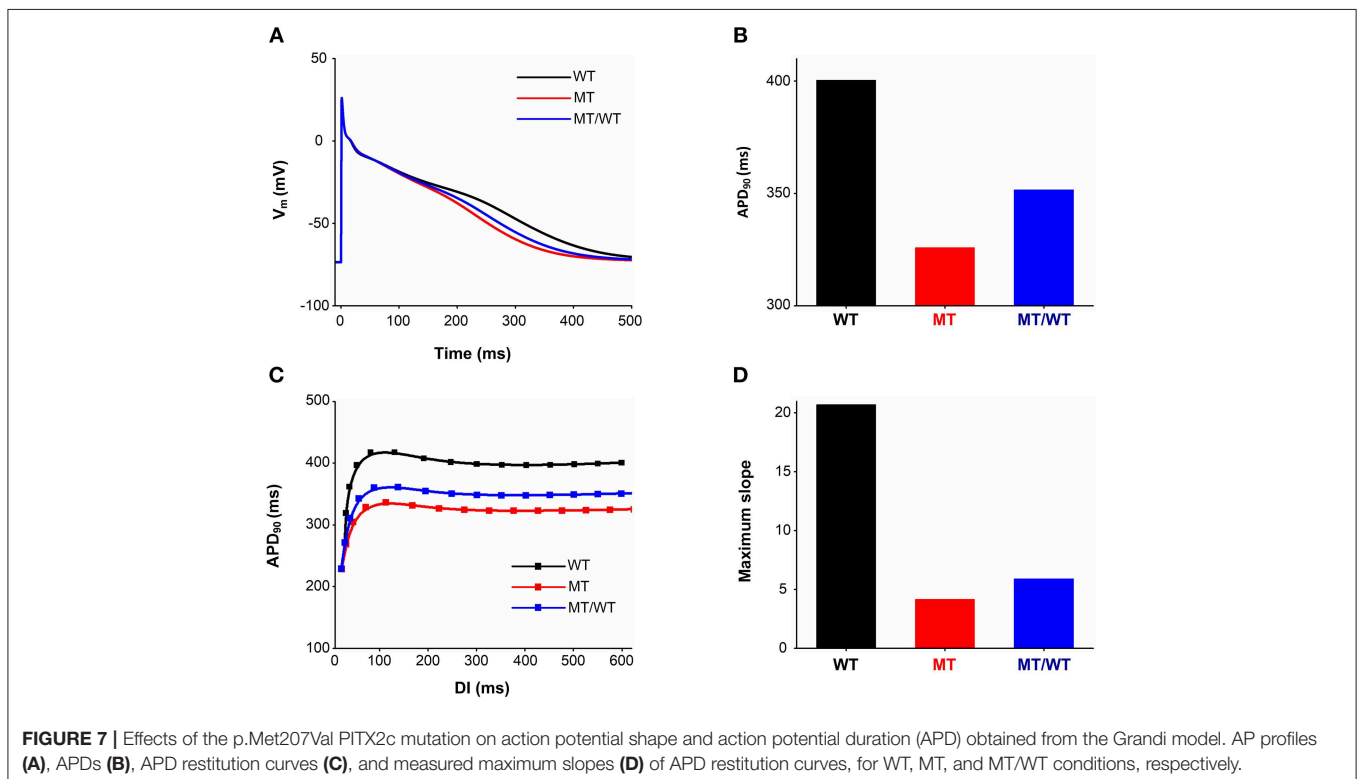
Model	Quantity	WT	MT/WT	MT
Cell	RMP (mV)	-81.49	-81.84	-81.98
	APA (mV)	104.23	104.39	104.46
	dV/dt _{max} (mV/ms)	199.92	199.26	199.07
	APD ₅₀ (ms)	123.36	77.61	61.26
	APD ₉₀ (ms)	260.62	197.58	170.14
	APD restitution slope	0.41	0.20	0.18
1D	CV (mm/ms)	0.269	0.237	0.230
	ERP (ms)	307.5	270.5	251.0
	WL (mm)	82.72	64.11	57.73
	Maximum rate (beats/min)	194	220	238
	VW (ms)	8.5	9.0	9.0
2D	Life span (ms)	<2,000	>5,000	>5,000
	Dominant frequency (Hz)	<4.0	5.4	10.0
	Minimal substrate size (mm)	54	47	36
	Tip meander area (cm ²)	2.904	1.198	0.469

Bold values represent parameters and characteristics under the p.Met207Val PITX2c mutation condition.

TABLE 3 | Quantitative characteristics of action potentials obtained from the Grandi model.

Quantity	WT	MT/WT	MT
RMP (mV)	-73.37	-73.50	-73.58
APA (mV)	99.19	99.62	99.83
dV/dt _{max} (mV/ms)	205.42	207.53	208.56
APD ₅₀ (ms)	136.04	127.44	122.04
APD ₉₀ (ms)	400.46	351.61	325.97

Bold values represent parameters and characteristics under the p.Met207Val PITX2c mutation condition.



other hand, the temporal vulnerability of atrial tissue is measured as VW during which unidirectional conduction block and re-entry can be induced by a test stimulus (Zhang et al., 2008; Kharche et al., 2012). In this study, the VW was significantly increased for atrial tissue incorporating remodeling due to the PITX2c p.Met207Val mutation. Consequently, the increase of temporal and spatial vulnerabilities of atrial tissues may explain why the PITX2c p.Met207Val mutation promotes initiation of re-entry.

In addition to AF initiation, the PITX2c p.Met207Val mutation promoted the maintenance of reentry by flattening the APD restitution curves. Steady-state APD is the principal determinant of the slope of the APD restitution curve. A recent study suggested factors that prolong the action potential would be expected to steepen the restitution curve (Shattock et al., 2017). In the present study, changes in I_{Ks} and I_{Kr} contribute to APD shortening and thereby flattened APD restitution curves. APD restitution has been proposed as a mechanistic determinant of the stability of re-entrant arrhythmia (Kharche et al., 2012; Shattock et al., 2017). In the case of the PITX2c p.Met207Val mutation, the maximum slope of the APD restitution curve was reduced. This led to a gradual decrease in APD alternans toward a steady state level and thereby a stable spiral wave at the tissue level. The stable spiral wave was characterized by decreased tip meander area and prolonged life span.

Therefore, the gain-of-function of the PITX2c p.Met207Val mutation promoted AF initiation and maintenance by abbreviating APD and slowing conduction.

Relevance to Previous Studies

Dysfunction of PITX2c predisposes to AF associated with both decreased (Wang et al., 2010; Chinchilla et al., 2011; Kirchhof et al., 2011; Kolek et al., 2014; Scridon et al., 2014; Tao et al., 2014; Aguirre et al., 2015; Lozano-Velasco et al., 2015, 2017; Herraiz-Martínez et al., 2018) and increased (Gore-Panter et al., 2014; Pérez-Hernández et al., 2015) expression (or activity) of PITX2c, and both loss- (Yang et al., 2013; Yuan et al., 2013; Zhou et al., 2013; Qiu et al., 2014; Wang et al., 2014; Wei et al., 2014) and gain-of-function of PITX2c mutations (Mechakra et al., 2019). Gain-of-function of PITX2c has previously been implicated in a marked shortening of the atrial APD and refractoriness (Pérez-Hernández et al., 2015). Overexpressed PITX2c increased the transcription of *KCNQ1* and *KCNE1* genes encoding I_{Ks} , and decreased I_{CaL} density through the atrial natriuretic peptide in human right atrial myocytes from chronic AF patients (Pérez-Hernández et al., 2015). Significantly, previous studies have reported that the I_{CaL} decrease (Van Wagoner et al., 1999) and the I_{Ks} increase (Voigt et al., 2010) critically contribute to the APD shortening (González de la Fuente et al., 2012). Recently, there has been increasing awareness of APD shortening due to malfunction of PITX2c in AF genesis (Kirchhof et al., 2011; Bai et al., 2018). Our data indicate that, in the case of the gain-of-function mutation p.Met207Val, the increase in I_{Ks} and I_{Kr} not only abbreviates APD, but also increases vulnerabilities of the atrial tissue to the initiation and maintenance of re-entry. Therefore, our study adds to the growing weight of

evidence implicating gain-of-function of PITX2c in increased susceptibility to AF.

Limitations

In this study, we used both CRN and Grandi models to simulate the AP of human atrial myocytes. Although these models were developed based on experimental data on human atrial myocytes and validated by their ability to reproduce APs and calcium transients, there were several limitations discussed elsewhere (Wilhelms et al., 2013; Voigt et al., 2014; Sutanto et al., 2018). Here, the limitations special to the present study are summarized. Firstly, the diffusion coefficient (D) was set to be $0.031 \text{ mm}^2/\text{ms}$ to make the tissue model fulfill the stability criterion ($D \frac{t}{x^2} < 0.5$) (Clayton and Panfilov, 2008; Kharche et al., 2012). Although the measured CV ($\sim 27 \text{ cm/s}$) is very close to realistic CVs (slow, 30 to 40 cm/s; normal 60 to 75 cm/s; and fast, 150 to 200 cm/s) (Gong et al., 2007), it is less than the human atrial CV under the normal condition (Kanagaratnam et al., 2002). Secondly, the potential impact of this mutation was evaluated under the following assumptions: (1) The PITX2c p.Met207Val mutation-induced functional changes in the proteins would be proportional to their mRNAs changes, and (2) These pro-arrhythmogenic effects would appear in human atrial cells as seen in HL1 cells. Further investigations should be conducted when more functional changes due to the PITX2c p.Met207Val mutation. Finally, the intrinsic heterogeneity, realistic geometry of the human atria and fiber orientation were not considered in this study, but these factors can influence the conduction of AP and may contribute to the genesis of spiral waves. The roles of these factors in AF were investigated in previous studies (Colman et al., 2013; Hansen et al., 2016; Zhao et al., 2017) and should not influence our conclusions. In fact, omitting these factors is useful to understand the mechanisms underlying reentrant arrhythmias arising from the PITX2c p.Met207Val mutation, in that changes in APD and spiral waves can be attributed with confidence to the implemented modifications to electrical components.

CONCLUSIONS

In this study, our findings add to the increasing weight of evidence implicating gain-of-function of PITX2c in increased susceptibility to the genesis and maintenance of familial AF, and further highlight the impact of electrical and structural remodeling in response to the PITX2c p.Met207Val mutation. In both heterozygous and homozygous forms of this mutation led to APD shortening due to ionic remodeling and slow conduction due to structural remodeling, which together increased tissue vulnerability to arrhythmogenesis. Therefore, we concluded that APD shortening and slow conduction may increase atrial susceptibility to atrial fibrillation arising from the PITX2c p.Met207Val mutation.

DATA AVAILABILITY STATEMENT

All datasets generated for this study are included in the manuscript/**Supplementary Files**.

AUTHOR CONTRIBUTIONS

JB, JZ, and HZ conceived and designed this work. JB conducted the experiments. JB, YL, AL, and HZ drafted the manuscript, interpreted the data, reviewed, revised, and approved the final version of this manuscript.

FUNDING

This work was supported by the National Natural Science Foundation of China (No. 61901192) (JB) and the Science

and Technology Planning Project of Guangdong Province (No. 2015B020214004 and No. 2015B020233010) (YL).

SUPPLEMENTARY MATERIAL

The Supplementary Material for this article can be found online at: <https://www.frontiersin.org/articles/10.3389/fphys.2019.01314/full#supplementary-material>

Supplementary Video 1 | Electrical waves under the WT condition.

Supplementary Video 2 | Electrical waves under the WT/MT condition.

Supplementary Video 3 | Electrical waves under the MT condition.

REFERENCES

- Aguirre, L., Alonso, M., Badía-Careaga, C., Rollán, I., Arias, C., Fernández-Mián, A., et al. (2015). Long-range regulatory interactions at the 4q25 atrial fibrillation risk locus involve PITX2c and ENPEP. *BMC Biol.* 13, 26–26. doi: 10.1186/s12915-015-0138-0
- Allessie, M. A., Bonke, F. I., and Schopman, F. J. (1977). Circus movement in rabbit atrial muscle as a mechanism of tachycardia. III. The “leading circle” concept: a new model of circus movement in cardiac tissue without the involvement of an anatomical obstacle. *Circ. Res.* 41, 9–18. doi: 10.1161/01.RES.41.1.9
- Bai, J., Gladding, P. A., Stiles, M. K., Fedorov, V. V., and Zhao, J. (2018). Ionic and cellular mechanisms underlying TBX5/PITX2 insufficiency-induced atrial fibrillation: insights from mathematical models of human atrial cells. *Sci. Rep.* 8:15642. doi: 10.1038/s41598-018-33958-y
- Bai, J., Wang, K., Li, Q., Yuan, Y., and Zhang, H. (2016a). Pro-arrhythmic effects of CACNA1C G1911R mutation in human ventricular tachycardia: insights from cardiac multi-scale models. *Sci. Rep.* 6:31262. doi: 10.1038/srep31262
- Bai, J., Wang, K., Liu, Y., Li, Y., Liang, C., Luo, G., et al. (2017a). Computational cardiac modeling reveals mechanisms of ventricular arrhythmogenesis in long QT syndrome type 8: CACNA1C R858H mutation linked to ventricular fibrillation. *Front. Physiol.* 8:771. doi: 10.3389/fphys.2017.00771
- Bai, J., Wang, K., and Zhang, H. (2016b). Potential pathogenesis discovery of arrhythmia based on cardiac electrophysiological models: research progress. *Progr. Biochem. Biophys.* 43, 128–140. doi: 10.16476/j.pibb.2015.0302
- Bai, J., Yin, R., Wang, K., and Zhang, H. (2017b). Mechanisms underlying the emergence of post-acidosis arrhythmia at the tissue level: a theoretical study. *Front. Physiol.* 8:195. doi: 10.3389/fphys.2017.00195
- Beauchamp, P., Yamada, K. A., Baertschi, A. J., Green, K., Kanter, E. M., Saffitz, J. E., et al. (2006). Relative contributions of connexins 40 and 43 to atrial impulse propagation in synthetic strands of neonatal and fetal murine cardiomyocytes. *Circ. Res.* 99, 1216–1224. doi: 10.1161/01.RES.0000250607.34498.b4
- Caballero, R., de la Fuente, M. G., Gómez, R., Barana, A., Amorós, I., Dolz-Gaitón, P., et al. (2010). In humans, chronic atrial fibrillation decreases the transient outward current and ultrarapid component of the delayed rectifier current differentially on each atria and increases the slow component of the delayed rectifier current in both. *J. Am. Coll. Cardiol.* 55, 2346–2354. doi: 10.1016/j.jacc.2010.02.028
- Chinchilla, A., Daimi, H., Lozano-Velasco, E., Dominguez, J. N., Caballero, R., Delpón, E., et al. (2011). PITX2 insufficiency leads to atrial electrical and structural remodeling linked to arrhythmogenesis. *Circ. Cardiovasc. Genet.* 4, 269–279. doi: 10.1161/CIRCGENETICS.110.958116
- Clayton, R., and Panfilov, A. (2008). A guide to modelling cardiac electrical activity in anatomically detailed ventricles. *Progr. Biophys. Mol. Biol.* 96, 19–43. doi: 10.1016/j.pbiomolbio.2007.07.004
- Colman, M. A., Aslanidi, O. V., Kharache, S., Boyett, M. R., Garratt, C., Hancox, J. C., et al. (2013). Pro-arrhythmic effects of atrial fibrillation-induced electrical remodelling: insights from the three-dimensional virtual human atria. *J. Physiol.* 591, 4249–4272. doi: 10.1113/jphysiol.2013.254987
- Courtemanche, M., Ramirez, R. J., and Nattel, S. (1998). Ionic mechanisms underlying human atrial action potential properties: insights from a mathematical model. *Am. J. Physiol. Heart Circ. Physiol.* 275, H301–H321. doi: 10.1152/ajpheart.1998.275.1.H301
- Dhillon, P. S., Chowdhury, R. A., Patel, P. M., Jabr, R., Momin, A. U., Vecht, J., et al. (2014). Relationship between connexin expression and gap junction resistivity in human atrial myocardium. *Circ. Arrhythm. Electrophysiol.* 7, 321–329. doi: 10.1161/CIRCEP.113.000606
- Fenton, F., and Karma, A. (1998). Vortex dynamics in three-dimensional continuous myocardium with fiber rotation: filament instability and fibrillation. *Chaos* 8, 20–47. doi: 10.1063/1.166311
- Gong, Y., Xie, F., Stein, K. M., Garfinkel, A., Cui, C. A., Lerman, B. B., et al. (2007). Mechanism underlying initiation of paroxysmal atrial flutter/atrial fibrillation by ectopic foci. *Circulation* 115, 2094–2102. doi: 10.1161/CIRCULATIONAHA.106.656504
- González de la Fuente, M., Barana, A., Gomez, R., Amorós, I., Dolz-Gaitón, P., Sacristan, S., et al. (2012). Chronic atrial fibrillation up-regulates β 1-adrenoceptors affecting repolarizing currents and action potential duration. *Cardiovasc. Res.* 97, 379–388. doi: 10.1093/cvr/cvs313
- Gore-Panter, S. R., Hsu, J., Hanna, P., Gillinov, A. M., Pettersson, G., Newton, D. W., et al. (2014). Atrial Fibrillation associated chromosome 4q25 variants are not associated with PITX2c expression in human adult left atrial appendages. *PLoS ONE* 9:e86245. doi: 10.1371/journal.pone.0086245
- Grandi, E., Pandit, S. V., Voigt, N., Workman, A. J., Dobrev, D., Jalife, J., et al. (2011). Human atrial action potential and Ca^{2+} model: sinus rhythm and chronic atrial fibrillation. *Circ. Res.* 109, 1055–1066. doi: 10.1161/CIRCRESAHA.111.253955
- Gudbjartsson, D. F., Arnar, D. O., Helgadóttir, A., Gretarsdóttir, S., Holm, H., Sigurdsson, A., et al. (2007). Variants conferring risk of atrial fibrillation on chromosome 4q25. *Nature* 448, 353–357. doi: 10.1038/nature06007
- Hansen, B. J., Csepe, T. A., Zhao, J., Ignozzi, A. J., Hummel, J. D., and Fedorov, V. V. (2016). Maintenance of atrial fibrillation. *Circ. Arrhythm. Electrophysiol.* 9:e004398. doi: 10.1161/CIRCEP.116.004398
- Hansen, B. J., Zhao, J., Csepe, T. A., Moore, B. T., Li, N., Jayne, L. A., et al. (2015). Atrial fibrillation driven by micro-anatomic intramural re-entry revealed by simultaneous sub-epicardial and sub-endocardial optical mapping in explanted human hearts. *Eur. Heart J.* 36, 2390–2401. doi: 10.1093/eurheartj/ehv233
- Heijman, J., Guichard, J.-B., Dobrev, D., and Nattel, S. (2018). Translational challenges in atrial fibrillation. *Circ. Res.* 122, 752–773. doi: 10.1161/CIRCRESAHA.117.311081
- Herráiz-Martínez, A., Llach, A., Tarifa, C., Gandía, J., Jiménez-Sabado, V., Lozano-Velasco, E., et al. (2018). The 4q25 variant rs13143308T links risk of atrial fibrillation to defective calcium homeostasis. *Cardiovasc. Res.* 115, 578–589. doi: 10.1093/cvr/cvy215
- Kanagaratnam, P., Rothery, S., Patel, P., Severs, N. J., and Peters, N. S. (2002). Relative expression of immunolocalized connexins 40 and 43 correlates with human atrial conduction properties. *J. Am. Coll. Cardiol.* 39, 116–123. doi: 10.1016/S0735-1097(01)01710-7

- Kanaporis, G., Kalik, Z. M., and Blatter, L. A. (2019). Action potential shortening rescues atrial calcium alternans. *J. Physiol.* 597, 723–740. doi: 10.1113/JP277188
- Kharache, S., Adeniran, I., Stott, J., Law, P., Boyett, M. R., Hancox, J. C., et al. (2012). Pro-arrhythmogenic effects of the S140G KCNQ1 mutation in human atrial fibrillation—insights from modelling. *J. Physiol.* 590, 4501–4514. doi: 10.1113/jphysiol.2012.229146
- Kirchhof, P., Kahr, P. C., Kaese, S., Piccini, I., Vokshi, I., Scheld, H.-H., et al. (2011). PITX2c is expressed in the adult left atrium, and reducing Pitx2c expression promotes atrial fibrillation inducibility and complex changes in gene expression. *Circ. Cardiovasc. Genet.* 4, 123–133. doi: 10.1161/CIRCGENETICS.110.958058
- Koivumäki, J. T., Seemann, G., Maleckar, M. M., and Tavi, P. (2014). *In silico* screening of the key cellular remodeling targets in chronic atrial fibrillation. *PLoS Comput. Biol.* 10:e1003620. doi: 10.1371/journal.pcbi.1003620
- Kolek, M. J., Parvez, B., Muhammad, R., Shoemaker, M. B., Blair, M. A., Stubblefield, T., et al. (2014). A common variant on chromosome 4q25 is associated with prolonged PR interval in subjects with and without atrial fibrillation. *Am. J. Cardiol.* 113, 309–313. doi: 10.1016/j.amjcard.2013.08.045
- Lozano-Velasco, E., Hernandez-Torres, F., Daimi, H., Serra, S. A., Herraiz, A., Hove-Madsen, L., et al. (2015). Pitx2 impairs calcium handling in a dose-dependent manner by modulating Wnt signalling. *Cardiovasc. Res.* 109, 55–66. doi: 10.1093/cvr/cvv207
- Lozano-Velasco, E., Wangenstein, R., Quesada, A., Garcia-Padilla, C., Osorio, J. A., Ruiz-Torres, M. D., et al. (2017). Hyperthyroidism, but not hypertension, impairs PITX2 expression leading to Wnt-microRNA-ion channel remodeling. *PLoS ONE* 12:e0188473. doi: 10.1371/journal.pone.0188473
- Mechakra, A., Footz, T., Walter, M., Aránega, A., Hernández-Torres, F., Morel, E., et al. (2019). A novel PITX2c gain-of-function mutation, p. Met207Val, in patients with familial atrial fibrillation. *Am. J. Cardiol.* 123, 787–793. doi: 10.1016/j.amjcard.2018.11.047
- Nao, T., Ohkusa, T., Hisamatsu, Y., Inoue, N., Matsumoto, T., Yamada, J., et al. (2003). Comparison of expression of connexin in right atrial myocardium in patients with chronic atrial fibrillation versus those in sinus rhythm. *Am. J. Cardiol.* 91, 678–683. doi: 10.1016/S0002-9149(02)03403-3
- Ni, H., Adeniran, I., and Zhang, H. (2017). *In-silico* investigations of the functional impact of KCNA5 mutations on atrial mechanical dynamics. *J. Mol. Cell. Cardiol.* 111, 86–95. doi: 10.1016/j.yjmcc.2017.08.005
- Nielsen, J. B., Thoroldsdottir, R. B., Fritsche, L. G., Zhou, W., Skov, M. W., Graham, S. E., et al. (2018). Genome-wide association study of 1 million people identifies 111 loci for atrial fibrillation. *bioRxiv* 2018:242149. doi: 10.1101/242149
- Pérez-Hernández, M., Matamoros, M., Barana, A., Amorós, I., Gómez, R., Núñez, M., et al. (2015). Pitx2c increases in atrial myocytes from chronic atrial fibrillation patients enhancing I_{Ks} and decreasing I_{Ca,L}. *Cardiovasc. Res.* 109, 431–441. doi: 10.1093/cvr/cvv280
- Polontchouk, L., Haefliger, J.-A., Ebel, B., Schaefer, T., Stuhlmann, D., Mehlhorn, U., et al. (2001). Effects of chronic atrial fibrillation on gap junction distribution in human and rat atria. *J. Am. Coll. Cardiol.* 38, 883–891. doi: 10.1016/S0735-1097(01)01443-7
- Qiu, X.-B., Xu, Y.-J., Li, R.-G., Xu, L., Liu, X., Fang, W.-Y., et al. (2014). PITX2C loss-of-function mutations responsible for idiopathic atrial fibrillation. *Clinics* 69, 15–22. doi: 10.6061/clinics/2014(01)03
- Scridon, A., Fouilloux-Meugnier, E., Loizon, E., Rome, S., Julien, C., Barrès, C., et al. (2014). Long-standing arterial hypertension is associated with Pitx2 down-regulation in a rat model of spontaneous atrial tachyarrhythmias. *Europace* 17, 160–165. doi: 10.1093/europace/euu139
- Seemann, G., Höper, C., Sachse, F. B., Dössel, O., Holden, A. V., and Zhang, H. (2006). Heterogeneous three-dimensional anatomical and electrophysiological model of human atria. *Philos. Transac. R. Soc. A Math. Phys. Eng. Sci.* 364, 1465–1481. doi: 10.1098/rsta.2006.1781
- Shattock, M. J., Park, K. C., Yang, H.-Y., Lee, A. W., Niederer, S., MacLeod, K. T., et al. (2017). Restitution slope is principally determined by steady-state action potential duration. *Cardiovasc. Res.* 113, 817–828. doi: 10.1093/cvr/cvx063
- Sossalla, S., Kallmeyer, B., Wagner, S., Mazur, M., Maurer, U., Toischer, K., et al. (2010). Altered Na⁺ currents in atrial fibrillation: effects of ranolazine on arrhythmias and contractility in human atrial myocardium. *J. Am. Coll. Cardiol.* 55, 2330–2342. doi: 10.1016/j.jacc.2009.12.055
- Sutanto, H., van Sloun, B., Schönleitner, P., van Zandvoort, M. A. M. J., Antoons, G., and Heijman, J. (2018). The subcellular distribution of ryanodine receptors and L-type Ca²⁺ channels modulates Ca²⁺-transient properties and spontaneous Ca²⁺-release events in atrial cardiomyocytes. *Front. Physiol.* 9:1108. doi: 10.3389/fphys.2018.01108
- Tao, Y., Zhang, M., Li, L., Bai, Y., Zhou, Y., Moon, A. M., et al. (2014). Pitx2, an atrial fibrillation predisposition gene, directly regulates ion transport and intercalated disc genes. *Circ. Cardiovasc. Genet.* 7, 23–32. doi: 10.1161/CIRCGENETICS.113.000259
- Van Wagoner, D. R., Pond, A. L., Lamorgese, M., Rossie, S. S., McCarthy, P. M., and Nerbonne, J. M. (1999). Atrial L-type Ca²⁺ currents and human atrial fibrillation. *Circ. Res.* 85, 428–436. doi: 10.1161/01.RES.85.5.428
- Voigt, N., Heijman, J., Wang, Q., Chiang, D. Y., Li, N., Karck, M., et al. (2014). Cellular and molecular mechanisms of atrial arrhythmogenesis in patients with paroxysmal atrial fibrillation. *Circulation* 129, 145–156. doi: 10.1161/CIRCULATIONAHA.113.006641
- Voigt, N., Trausch, A., Knaut, M., Matschke, K., Varró, A., Van Wagoner, D. R., et al. (2010). Left-to-right atrial inward rectifier potassium current gradients in patients with paroxysmal versus chronic atrial fibrillation. *Circ. Arrhythm. Electrophysiol.* 3, 472–480. doi: 10.1161/CIRCEP.110.954636
- Wang, J., Klysiak, E., Sood, S., Johnson, R. L., Wehrens, X. H., and Martin, J. F. (2010). Pitx2 prevents susceptibility to atrial arrhythmias by inhibiting left-sided pacemaker specification. *Proc. Natl. Acad. Sci. U.S.A.* 107, 9753–9758. doi: 10.1073/pnas.0912585107
- Wang, J., Zhang, D.-F., Sun, Y.-M., and Yang, Y.-Q. (2014). A novel PITX2c loss-of-function mutation associated with familial atrial fibrillation. *Eur. J. Med. Genet.* 57, 25–31. doi: 10.1016/j.ejmg.2013.11.004
- Wei, D., Gong, X.-H., Qiu, G., Wang, J., and Yang, Y.-Q. (2014). Novel PITX2c loss-of-function mutations associated with complex congenital heart disease. *Int. J. Mol. Med.* 33, 1201–1208. doi: 10.3892/ijmm.2014.1689
- Wetzel, U., Boldt, A., Lauschke, J., Weigl, J., Schirdewahn, P., Dorszewski, A., et al. (2005). Expression of connexins 40 and 43 in human left atrium in atrial fibrillation of different aetiologies. *Heart* 91, 166–170. doi: 10.1136/hrt.2003.024216
- Whittaker, D., Colman, M. A., Ni, H., Hancox, J., and Zhang, H. (2018a). Human atrial arrhythmogenesis and sinus bradycardia in KCNQ1-linked short QT syndrome: insights from computational modelling. *Front. Physiol.* 9:1402. doi: 10.3389/fphys.2018.01402
- Whittaker, D. G., Hancox, J., and Zhang, H. (2018b). *In silico* assessment of pharmacotherapy for human atrial patho-electrophysiology associated with hERG-linked short QT syndrome. *Front. Physiol.* 9:1888. doi: 10.3389/fphys.2018.01888
- Whittaker, D. G., Ni, H., El Harchi, A., Hancox, J. C., and Zhang, H. (2017). Atrial arrhythmogenicity of KCNJ2 mutations in short QT syndrome: insights from virtual human atria. *PLoS Comput. Biol.* 13:e1005593. doi: 10.1371/journal.pcbi.1005593
- Wiener, N. (1946). The mathematical formulation of the problem of conduction of impulses in a network of connected excitable elements, specifically in cardiac muscle. *Arch. Inst. Cardiol. Mex.* 16, 1–61.
- Wilhelms, M., Hettmann, H., Maleckar, M., Koivumäki, J., Dössel, O., and Seemann, G. (2013). Benchmarking electrophysiological models of human atrial myocytes. *Front. Physiol.* 3:487. doi: 10.3389/fphys.2012.00487
- Yang, Y.-Q., Xu, Y.-J., Li, R.-G., Qu, X.-K., Fang, W.-Y., and Liu, X. (2013). Prevalence and spectrum of PITX2c mutations associated with familial atrial fibrillation. *Int. J. Cardiol.* 168, 2873–2876. doi: 10.1016/j.ijcard.2013.03.141
- Yuan, F., Zhao, L., Wang, J., Zhang, W., Li, X., Qiu, X.-B., et al. (2013). PITX2c loss-of-function mutations responsible for congenital atrial septal defects. *Int. J. Med. Sci.* 10, 1422–1429. doi: 10.7150/ijms.6809
- Zhang, H., Kharache, S., Holden, A. V., and Hancox, J. C. (2008). Repolarisation and vulnerability to re-entry in the human heart with short QT syndrome arising

- from KCNQ1 mutation—A simulation study. *Progr. Biophys. Mol. Biol.* 96, 112–131. doi: 10.1016/j.pbiomolbio.2007.07.020
- Zhao, J., Hansen, B. J., Wang, Y., Csepe, T. A., Sul, L. V., Tang, A., et al. (2017). Three dimensional integrated functional, structural, and computational mapping to define the structural fingerprints of heart specific atrial fibrillation drivers in human heart *ex vivo*. *J. Am. Heart Assoc.* 6:e005922. doi: 10.1161/JAHA.117.005922
- Zhou, Y. M., Zheng, P. X., Yang, Y. Q., Ge, Z. M., and Kang, W. Q. (2013). A novel PITX2c loss-of-function mutation underlies lone atrial fibrillation. *Int. J. Mol. Med.* 32, 827–834. doi: 10.3892/ijmm.2013.1463

Conflict of Interest: The authors declare that the research was conducted in the absence of any commercial or financial relationships that could be construed as a potential conflict of interest.

Copyright © 2019 Bai, Lu, Lo, Zhao and Zhang. This is an open-access article distributed under the terms of the Creative Commons Attribution License (CC BY). The use, distribution or reproduction in other forums is permitted, provided the original author(s) and the copyright owner(s) are credited and that the original publication in this journal is cited, in accordance with accepted academic practice. No use, distribution or reproduction is permitted which does not comply with these terms.